Scientia Iranica B (2020) 27(5), 2465–2477

Sharif University of Technology
Scientia Iranica
Transactions B: Mechanical Engineering
http://scientiairanica.sharif.edu

Series solution of slip flow of Al_2O_3 and Fe_3O_4 nanoparticles in a horizontal channel with a porous medium by using least square and Galerkin methods

Z. Abbas[a], J. Hasnain[b,*], M. Aqeel[a], I. Mustafa[c], and A. Ghaffari[d]

a. *Department of Mathematics, The Islamia University of Bahawalpur, Bahawalpur 63100, Pakistan.*
b. *Department of Computer Sciences, Bahria University Islamabad Campus, Islamabad 44000, Pakistan.*
c. *Department of Mathematics, Allama Iqbal Open University, Islamabad 44000, Pakistan.*
d. *Department of Mathematics, University of Education, Attock Campus, 43600, Pakistan.*

Received 31 January 2019; received in revised form 8 May 2019; accepted 13 July 2019

KEYWORDS
Semi-porous channel;
Nanofluid;
Porous medium;
Slip effects;
Series solution.

Abstract. This study theoretically investigates the effects of slip on the two-dimensional flow of nano liquid in a semi-porous channel, which is designed by two long rectangular plates having porous media. One of the channel walls is porous and the other rigid and slippery. A transverse magnetic field characterized by homogeneous strength was applied to the flow direction. Magnetic nanoparticles (Fe_3O_4) and non-magnetic nanoparticles (Al_2O_3) were considered with Ethylene Glycol (EG) and water as Base Fluids (BFs). Least Square Method (LSM) and Galerkin Method (GM) were adopted to solve those equations that were transformed from partial Differential Equations (DEs) to ordinary ones by Berman's similarity transformations. The obtained results of the two analytical methods were compared with those of the fourth-order Runge-Kutta Numerical Method (NM). Based on a comparison of GM and LSM, although the variation in velocity profiles was quite insignificant, the accuracy of GM was higher than LSM. The contributions of various flow parameters were depicted in graphs. Results showed a decrement in the fluid velocity with an increase in the slip and porosity parameters. The fluid boundary layer decreased as the Reynolds number increased. Flow field for magnetic nanoparticles is less than that for nonmagnetic particles.

1. Introduction

In recent years, numerous applications of biomedical engineering have shifted academic attention to flow problems in porous tubes/channels, examples of which include blood flow in the capillaries [1], blood flow in oxygenator [2], and blood dialysis in artificial kidney [3]. Engineering applications include filter designing [4], diffusion of gases [5], and transpiration cooling control of the Boundary Layer (BL) [6]. In 1953, Berman [7] solved the Navier-Stokes equation, describing the flow phenomenon of viscous fluid through a rectangular cross-section with porous walls. The flow of viscous fluid exposed to an external magnetic field and streaming in a channel with one porous wall was analyzed by Sheikholeslami et al. [8].

The unique features of nanotechnology have drawn much attention as it provides diverse perspectives on and approaches to modeling and composing products with efficient heat transport enhancements. An approach to improving heat transfer attributes of fluids is the dissemination of nano-sized particles into the low thermal conductive liquids like water,

*. *Corresponding author. Tel.: +92 51 9263268*
E-mail address: jafar_hasnain14@yahoo.com (J. Hasnain)

doi: 10.24200/sci.2019.52830.2904

kerosene, Ethylene Glycol (EG), and oil. This newly found class of fluids, initially established by Choi et al. [9,10], enjoys exclusive physical and chemical properties. A few instances of its applications include lubricants, cooling and heating of buildings, engine transmission of oil, the cooling system in nuclear plants, microchannel cooling, and chemical process. One of the fluids belonging to this class is ferrofluid which comprises ferrum like Fe_3O_4. These particles are temporarily magnetized by the application of magnetic force; however, their behavior is like usual metallic particles in the absence of magnetic force. These fluids possess magnetic properties of solid and fluid characteristics of liquid. These characteristics make such fluids widely applicable, instances of which include viscous damper for gravity gradient satellites, rotating anode X-ray generators, energy conversion devices, magnetic cell separation, and magnetic drug targeting. Studies on nanofluid flow with different flow geometries are listed [11–27].

Suction/injection of fluid through the boundary of the system can considerably affect its flow. Usually, coefficients of skin friction are reduced due to injection, while they experience an increase due to suction [28–30].

Weighted Residual Methods (WRMs) such as Collocation Method (CM), Least Square Method (LSM), and Galerkin Method (GM) are accurate and easy approximation techniques that are used to solve DEs. To find a solution to a third-order linear DE, CM was proposed by Rasmussen and Stern [31]. Another solution method among WRMs is Orthogonal method and Vaferi et al. [32] applied it to the diffusivity equation in their study on radial transient flow. To predict how the longitudinal fin performs, Aziz and Bouaziz [33,34] found that the LSM was the simplest method of all the WRMs.

This paper analyzes electrically conducting nanofluid flow in a channel suffused with porous media. It is assumed that one plate of the channel is porous and the other rigid. Darcy's law is applied to studying the effects of the porous medium, while Navier slip is applied at the lower wall to examine the impact of slip on the fluid flow. By invoking the dimensionless variables, the resulting governing DEs are reduced to coupled and non-linear ordinary DEs. Solutions to the coupled non-linear equations are obtained by using WRM. The behavior of velocity profiles under the effect of involved parameters is presented in graphs and tables.

2. Description of the problem

The fluid under consideration is confined to a region between two parallel plates with a distance h (see Figure 1). A rigid infinite plate of length L_x is placed along x^*-axis at $y^* = 0$ where the slip condition is applied; however, the other infinite plate is porous at which the transpiration velocity is q The flow inside the channel occupied with porous media is steady, laminar and two-dimensional with constant physical properties of fluid. Two different Base Fluids (BFs), namely water and kerosene, are considered that carry magnetite (Fe_3O_4) and alumina (Al_2O_3) as nanoparticles. The intensity B of a homogenous magnetic field is considered which is imposed transversely on the flow direction. Assumption of low magnetic Reynolds number is also taken into account due to which induced magnetic field is neglected. The equations governing the flow phenomenon under the aforesaid assumptions are as follows [30]:

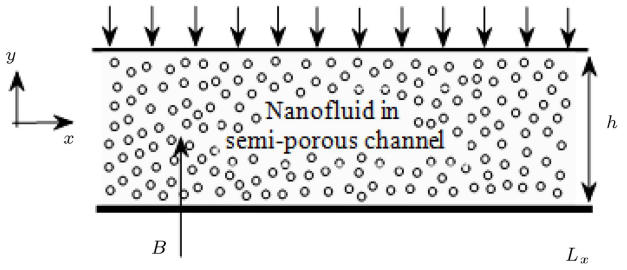

Figure 1. Schematic diagram of flow model.

$$\frac{\partial \tilde{u}}{\partial \tilde{x}} + \frac{\partial \tilde{v}}{\partial \tilde{y}} = 0, \tag{1}$$

$$\tilde{u}\frac{\partial \tilde{u}}{\partial \tilde{x}} + \tilde{v}\frac{\partial \tilde{u}}{\partial \tilde{y}} = -\frac{1}{\rho_{nf}}\frac{\partial \tilde{P}}{\partial \tilde{x}} + \frac{\mu_{nf}}{\rho_{nf}} \left(\frac{\partial^2 \tilde{u}}{\partial \tilde{x}^2} + \frac{\partial^2 \tilde{u}}{\partial \tilde{y}^2}\right) - \tilde{u}\frac{\sigma_{nf}B^2}{\rho_{nf}} - \frac{1}{k_1}\frac{\mu_{nf}}{\rho_{nf}}\tilde{u}, \tag{2}$$

$$\tilde{u}\frac{\partial \tilde{v}}{\partial \tilde{x}} + \tilde{v}\frac{\partial \tilde{v}}{\partial \tilde{y}} = -\frac{1}{\rho_{nf}}\frac{\partial \tilde{P}}{\partial \tilde{y}} + \frac{\mu_{nf}}{\rho_{nf}}\left(\frac{\partial^2 \tilde{v}}{\partial \tilde{x}^2} + \frac{\partial^2 \tilde{v}}{\partial \tilde{y}^2}\right), - \frac{1}{k_1}\frac{\mu_{nf}}{\rho_{nf}}\tilde{v}. \tag{3}$$

Effective density is determined through the following relation [30]:

$$\rho_{nf} = \rho_f(1-\phi) + \rho_s\phi,$$

where ϕ is the nanoparticle volume fraction. The dynamic viscosity of nanofluids for two different models [30] is given in Table 1. The thermo-physical properties of nanoparticles and conventional fluids are given in Table 2.

The allied boundary conditions are given below:

$$\tilde{u}(0) = u_0 + l\frac{\partial \tilde{u}}{\partial \tilde{y}}, \qquad \tilde{v}(0) = 0,$$

$$\tilde{u}(h) = 0, \qquad \tilde{v}(h) = -q, \tag{4}$$

Table 1. Different models for calculation of dynamic viscosities.

Model	Electrical conductivity	Dynamic viscosity
I	$\frac{\sigma_{nf}}{\sigma_f} = 1 + \frac{3\left(\frac{\sigma_s}{\sigma_f} - 1\right)\phi}{\left(\frac{\sigma_s}{\sigma_f} + 2\right) - \left(\frac{\sigma_s}{\sigma_f} - 1\right)\phi}$	$\mu_{nf} = \frac{\mu_f}{(1-\phi)^{2.5}}$
II	$\frac{\sigma_{nf}}{\sigma_f} = 1 + \frac{3\left(\frac{\sigma_s}{\sigma_f} - 1\right)\phi}{\left(\frac{\sigma_s}{\sigma_f} + 2\right) - \left(\frac{\sigma_s}{\sigma_f} - 1\right)\phi}$	$\mu_{nf} = \mu_f\left(1 + 7.3\phi + 123\phi^2\right)$

Table 2. Thermo physical properties of magnetic nanoparticles and base fluids [14,23].

Material	ρ (kg/m^3)	Electrical conductivity $\sigma\ ((\Omega \cdot \mathrm{m})^{-1})$
Fe_3O_4	5200	25.000
Al_2O_3	3970	3.5×10^7
Ethylene Glycol (EG)	1113.2	1.07×10^{-4}
Drinking water	997.1	0.05

where l is the length of slip and no slip is recovered at $l = 0$. The velocity slip at the plate was introduced by Navier and named as Navier slip condition. The researchers [35–38] used this condition due to its implementation in several industrial and engineering processes where the flow is confined by pipes, walls, and curved surfaces.

The mean velocity U can be computed through the following relation:

$$Uh = \int_0^h \tilde{u} d\tilde{y} = L_x q. \tag{5}$$

The following dimensionless variables are used as follows:

$$x = \frac{\tilde{x}}{L_x}, \qquad y = \frac{\tilde{y}}{h}, \qquad u = \frac{\tilde{u}}{U},$$

$$v = \frac{\tilde{v}}{q}, \qquad P_y = \frac{\tilde{p}}{\rho q^2}. \tag{6}$$

In a dimensionless form, Eqs. (1) to (3) become:

$$\frac{\partial u}{\partial x} + \frac{\partial v}{\partial y} = 0, \tag{7}$$

$$u\frac{\partial u}{\partial x} + v\frac{\partial u}{\partial y} = -\varepsilon^2 \frac{\partial P_y}{\partial x} + \frac{\mu_{nf}}{hq\rho_{nf}}\left(\varepsilon^2 \frac{\partial^2 u}{\partial x^2} + \frac{\partial^2 u}{\partial y^2}\right) - u\frac{Ha^2 B*}{\mathrm{Re}A*} - u\frac{\lambda}{\mathrm{Re}A*(1-\phi)^{2.5}}, \tag{8}$$

$$u\frac{\partial v}{\partial x} + v\frac{\partial v}{\partial y} = -\frac{\partial P_y}{\partial y} + \frac{\mu_{nf}}{\rho_{nf}}\frac{1}{hq}\left(\varepsilon^2 \frac{\partial^2 v}{\partial x^2} + \frac{\partial^2 v}{\partial y^2}\right) - v\frac{\mu_{nf}}{\rho_{nf}}\frac{\lambda}{hq}, \tag{9}$$

where the nondimensional parameter for magnetic forces is the Hartmann number $\mathrm{Ha} = Bh\sqrt{\sigma_f/\rho_f \upsilon_f}$, for dynamic forces is the Reynolds number $\mathrm{Re} = hq/\nu_f$, and for porosity is $\lambda = h^2/k_1$; the constants A^* and B^* are as follows:

$$A^* = \frac{\rho_{nf}}{\rho_f} = (1-\phi) + \frac{\rho_s}{\rho_f}\phi,$$

$$B^* = \frac{\sigma_{nf}}{\sigma_f} = 1 + \frac{3\left(\frac{\sigma_s}{\sigma_f} - 1\right)\phi}{\left(\frac{\sigma_s}{\sigma_f} + 2\right) - \left(\frac{\sigma_s}{\sigma_f} - 1\right)\phi}. \tag{10}$$

In Eqs. (8) and (9), the term ε is very small as it is the ratio of the distance h to the length L_x of the slider. To eliminate the aspect ratio ε, Berman's similarity transformations [7] are used as follows:

$$v = -V(y), \quad y = \frac{\tilde{y}}{h},$$

$$u = \frac{\tilde{u}}{U} = u_0 U(y) + x\frac{dV}{dy}. \tag{11}$$

Application of the above relations to Eq. (9) shows that the quantity $\partial P_y/\partial y$ is independent of x. Besides, according to Eq. (8), it is found that $\partial^2 P_y/\partial x^2$ is not a function of x. In channel, flow becomes a fully developed laminar flow when velocity profile remains unchanged in the axial direction and is then converted into a similar problem. For simplicity, the asterisks are ignored and after separating the variables, one gets:

$$\left(V'(y)\right)^2 - V(y)V''(y) - \frac{1}{\mathrm{Re}A*(1-\phi)^{2.5}}V'''(y) + \frac{\mathrm{Ha}^2 B*}{\mathrm{Re}A*}V'(y) + \frac{1}{\mathrm{Re}}\frac{\lambda}{A*(1-\phi)^{2.5}}V'(y) = \varepsilon^2\frac{\partial^2 P_y}{\partial x^2} = -\varepsilon^2\frac{1}{x}\frac{\partial P_y}{\partial x}, \tag{12}$$

$$U(y)V'(y) - V(y)U'(y) = \frac{1}{\mathrm{Re}A * (1-\phi)^{2.5}} \left[U''(y) - \mathrm{Ha}^2 B * (1-\phi)^{2.5} U(y) - \lambda U(y)\right]. \quad (13)$$

Further differentiation of Eq. (12) with respect to y gives:

$$V^{IV}(y) = \mathrm{Ha}^2 B * (1-\phi)^{2.5} V''(y) + \mathrm{Re}A * (1-\phi)^{2.5}[V'(y)V''(y) - V(y)V'''(y)] + \lambda V''(y). \quad (14)$$

The boundary conditions in the dimensionless form are:

$$U(0) = 1 + \beta U'(0), \quad V(0) = 0, \quad V'(0) = \beta V''(0),$$
$$U(1) = 0, \quad V(1) = 1, \quad V'(1) = 0. \quad (15)$$

Here, $\beta = \frac{l}{h}$ is the slip parameter.

3. Weighted Residual Method (WRM)

Weighted residual technique is an approximation technique and is the most useable procedure applicable to nonlinear dynamical models. Sometimes, this method is quite accurate at initial guesses, which successively improves the approximation [39]. The approximate solution in the analytical form often becomes more useful than the numerical solution and shorter computation time is required to generate an approximate solution. This method is very easy to apply as compared to other analytical methods such as homotopy analysis method. The principal objective of WRMs is to obtain an approximate solution to the DE.

Consider a differential operator:

$$D(F) = f, \quad (16)$$

subjected to the boundary conditions:

$$B_j F = g_j. \quad (17)$$

To find an approximate solution to the given boundary value problem, consider a linear combination (linearly independent) of basic functions as follows:

$$\hat{F} = F_0 + \sum_{j=1}^{m} c_j \phi_j, \quad (18)$$

where F_0 is chosen such that it must satisfy the boundary conditions, completely if possible. ϕ_j represents the linearly independent functions called trial functions, which are supposed to be known, and coefficients c_j are the unknowns and can be obtained by solving a system of equations.

Substitution of Eq. (18) into Eq. (16) will not satisfy the equation. Hence, an error or residual R which is a continuous function of spatial coordinates will exist and is written as follows:

$$R = D\left(\hat{F}\right) - f \neq 0. \quad (19)$$

At one spatial coordinate, the approximating functions may be the trigonometric functions or the polynomials, which are given in the following form:

$$\phi_j(x) = x^{j-1} \quad \text{or} \quad \phi_j(x) = \sin j\pi x. \quad (20)$$

The objective of WRM is to make the error or the residual equal to zero over the whole domain in an average sense. That is:

$$\int_X R(x) W_j(x) dx = 0, \qquad j = 1, 2, 3, ..., m, \quad (21)$$

where the number of Weight Functions (WFs) is exactly equal to the unknown coefficients c_j. There are many methods to choose the WF, called test function. Two methods of the WRMs to choose the WF are described below in the following subsections.

3.1. Least Square Method (LSM)

In this method, the sum of square of residuals is assumed rather than the sum of residuals and it is minimized to obtain the minimum value as follows:

$$E = \int_X R(x)R(x)dx = \int_X R^2(x)dx. \quad (22)$$

Now, to determine the minimum of the given function, Eq. (22) is differentiated with respect to the unknown constants c_j and these derivatives are set equal to zero. That is,

$$\frac{\partial E}{\partial c_j} = 2\int_X R(x)\frac{\partial R}{\partial c_j}dx = 0, \quad j = 1, 2, 3, ..., m. \quad (23)$$

After comparing Eq. (23) with Eq. (21), the WFs are:

$$W_j = 2\frac{\partial R}{\partial c_j}. \quad (24)$$

Coefficient "2" can be ignored because it is absorbed into the equation. Therefore, the WFs in this method are only the derivatives of the residuals R with respect to the unknown constants c_j, that is:

$$W_j = \frac{\partial R}{\partial c_j}. \quad (25)$$

3.2. Galerkin Method (GM)

GM is better than the LSM. Galerkin technique is the modified form of LSM. In this method, to find the WFs, we take the derivatives of the trial functions with respect to the unknowns c_j rather than the derivatives of the residuals to the unknowns. Therefore, the WFs in this method are given below:

$$W_j = \frac{\partial \hat{F}}{\partial c_j}, \qquad j = 1, 2, 3, ..., m. \quad (26)$$

4. Solution

By using Eq. (18), the trial functions satisfying the boundary conditions given in Eqs. (15) are:

$$U(y) = \frac{1}{1+\beta}\Big(1 - y + c_1\left(-\beta - y + y^2(1+\beta)\right) + c_2\left(-\beta - y + y^3(1+\beta)\right) + c_3\left(-\beta - y + y^4(1+\beta)\right)\Big),$$

$$V(y) = \frac{6\beta y}{(1+4\beta)} + \frac{3y^2}{(1+4\beta)} - \frac{(2+2\beta)\,y^3}{(1+4\beta)} + c_4\begin{pmatrix}\frac{2\beta y}{(1+4\beta)} + \frac{y^2}{(1+4\beta)} \\ -\frac{2y^3(1+3\beta)}{(1+4\beta)} + y^4\end{pmatrix} + c_5\left(\frac{4\beta y}{(1+4\beta)} + \frac{2y^2}{(1+4\beta)} - \frac{y^3\,(3+8\beta)}{(1+4\beta)} + y^5\right). \quad (27)$$

Substitution of Eq. (27) into Eqs. (13) and (14) gives the two following residuals: $R_1(c_1 - c_5, y)$ and $R_2(c_1 - c_5, y)$. Next, LSM and GM are applied to determine the unknowns $(c_1 - c_5)$ for $U(y)$ and $V(y)$.

4.1. Least Square Method (LSM)

After applying Eq. (25), WFs are obtained. Substitution of these functions along with residuals into Eq. (21) gives a system of five nonlinear equations in five unknowns $(c_1 - c_5)$. By using Newton's method, this system can be solved for unknowns $(c_1 - c_5)$. Finally, the trial functions $U(y)$ and $V(y)$ for water-Fe_3O_4 nanofluid with Re=1, Ha=1, $\beta = 0.1$, $\lambda = 0.1$, and $\phi = 0.05$ are obtained by Eq. (28) as shown in Box I.

4.2. Galerkin Method (GM)

Similarly, GM is used for determining trial functions $U(y)$ and $V(y)$. The WFs are determined through Eq. (26):

$$W_1' = \frac{\partial U}{\partial c_1} = \left(\frac{\beta + y - y^2\,(1+\beta)}{1+\beta}\right),$$

$$W_2' = \frac{\partial U}{\partial c_2} = \left(\frac{\beta + y - y^3\,(1+\beta)}{1+\beta}\right),$$

$$W_3' = \frac{\partial U}{\partial c_3} = \left(\frac{2y\beta + y^2}{1+2\beta}\right),$$

$$W_4' = \frac{\partial V}{\partial c_4} = \left(\frac{2y\beta + y^2}{1+2\beta} + \frac{2y^3\,(1+3\beta)}{1+4\beta} - y^4\right),$$

$$W_5' = \frac{\partial V}{\partial c_5} = \left(\frac{2y\beta + y^2}{1+2\beta} + \frac{y^3\,(3+8\beta)}{1+4\beta} - y^5\right). \quad (29)$$

Substituting the above weights with residuals into Eq. (21) gives a system of five nonlinear equations with five unknowns $(c_1 - c_5)$. Newton's method is applied to linearize the nonlinear system and solve it for unknowns $(c_1 - c_5)$. Then, the trial functions $U(y)$ and $V(y)$ for water-Fe_3O_4 nanofluid having Re = 1, Ha = 1, $\beta = 0.1$, $\lambda = 0.1$, and $\phi = 0.05$, are obtained by Eq. (30) as shown in Box II.

5. Results and discussion

LSM and GM are used to obtain the solution to flow equations of Magnetohydrodynamics (MHD) nanofluid in a channel with one permeable wall and the other having slippery surface suffused with a porous medium. For comparison purposes, the flow equations are also solved numerically. Eqs. (13) and (14) are solved along with Condition (15) and the comparison is analyzed in graphs and tables by using different nanofluid arrangements (Table 1).

Figure 2(a) and (b) shows a comparison of the results of the applied methods for, respectively. The results obtained from LSM and GM show that the difference of the velocity profiles is almost insignificant and, thus, can be ignored. According to the figures, the results obtained by GM are closer to those by the numerical method than to the LSM.

Figure 3(a) and (b) shows the impact of porosity parameter λ on $U(y)$ and $V'(y)$ in the presence and absence of slip effects for water-Fe_3O_4 nanofluid using $\phi = 0.05$, Ha = 1, and Re = 1 From these figures, as λ increases, the thickness of velocity BL and fluid velocity are reduced. The rise of the porosity parameter physically improves the damping force on the fluid's speed that leads to a decrease in the speed of fluid. The fluid velocity is also reduced with an increment in the slip parameter.

$$U(y) = 0.909091\left(-0.0956253\begin{pmatrix}1.1y^4- \\ y-0.1\end{pmatrix} - 0.0238745\begin{pmatrix}1.1y^3- \\ y-0.1\end{pmatrix} + 0.783669\begin{pmatrix}1.1y^2- \\ y-0.1\end{pmatrix} - y + 1\right),$$

$$V(y) = 0.714286\left(-2.2y^3 + 3y^2 - 0.0623305\begin{pmatrix}1.4y^5 - 3.8y^3 \\ +2y^2 + 0.4y\end{pmatrix} + 0.337334\begin{pmatrix}1.4y^4 - 2.6y^3 \\ +y^2 + 0.2y\end{pmatrix} + 0.6y\right). \quad (28)$$

Box I

$$U(y) = 0.909091\left(-0.108639\begin{pmatrix}1.1y^4-\\ y-0.1\end{pmatrix} - 0.0161103\begin{pmatrix}1.1y^3-\\ y-0.1\end{pmatrix} + 0.793533\begin{pmatrix}1.1y^2-\\ y-0.1\end{pmatrix} - y + 1\right),$$

$$V(y) = 0.714286\left(-2.2y^3 + 3y^2 - 0.0795448\begin{pmatrix}1.4y^5 - 3.8y^3\\ +2y^2 + 0.4y\end{pmatrix} + 0.369404\begin{pmatrix}1.4y^4 - 2.6y^3\\ +y^2 + 0.2y\end{pmatrix} + 0.6y\right). \quad (30)$$

Box II

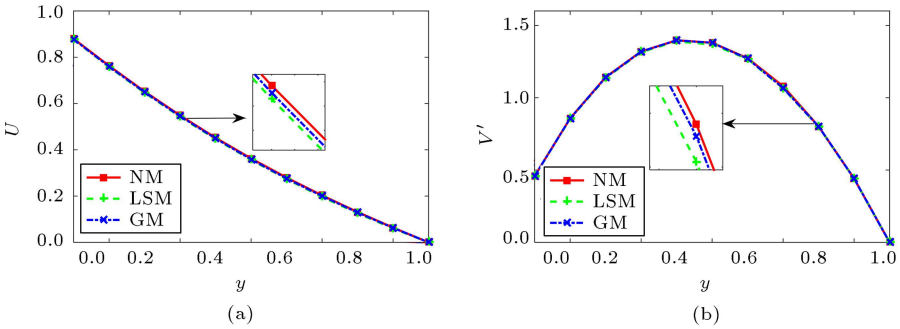

Figure 2. Comparison of (a) $U(y)$ and (b) $V'(y)$ by the applied methods with Ha = 1, Re = 1, $\lambda = 0.1$, $\beta = 0.1$ and $\phi = 0.05$ in case of water-Fe_3O_4 nanofluid.

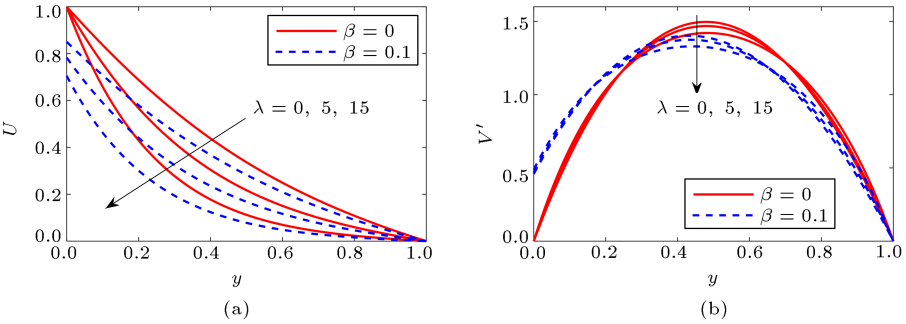

Figure 3. (a) $U(y)$ and (b) $V'(y)$ for λ with Ha = 1, Re = 1, and $\phi = 0.05$ for water-Fe_3O_4 nanofluid.

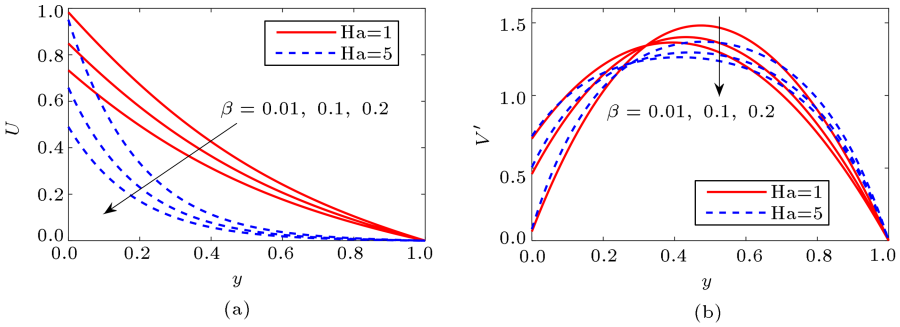

Figure 4. (a) $U(y)$ and (b) $V'(y)$ for β with $\lambda = 0.1$, Re = 1, and $\phi = 0.05$ for water-Fe_3O_4 nanofluid.

The slip effects with two different values of Hartman number on $U(y)$ and $V'(y)$ for water-Fe_3O_4 nanofluid are plotted in Figure 4(a) and (b). These figures show significant effect of the slip parameter on the velocity profiles. It can also be noticed that as the Hartman number increases, the slip effects remain significant. Moreover, the velocity BL decreases at higher values of the Hartman number, according to Figure 4(a). From Figure 4(b), it can be noticed that $V'(y)$ initially increases with rise in the slip parameter, while it decreases at a distance closer to the upper plate.

Figure 5(a) and (b) gives the effect of Re on $U(y)$ and $V'(y)$ for water-Fe_3O_4 nanofluid with and without

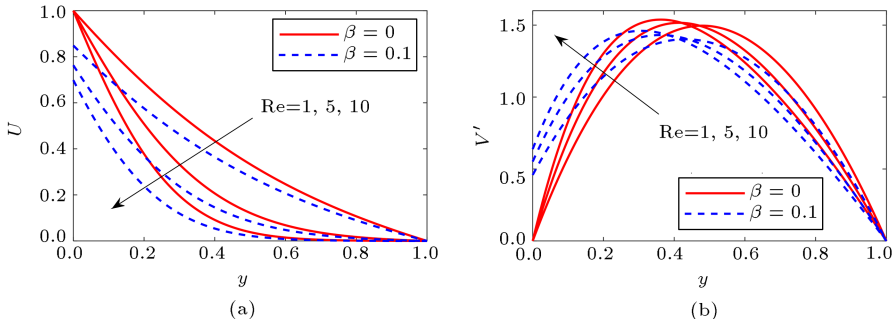

Figure 5. (a) $U(y)$ and (b) $V'(y)$ for Re with $\lambda = 0.1$, Ha $= 1$, and $\phi = 0.05$ for water-Fe_3O_4 nanofluid.

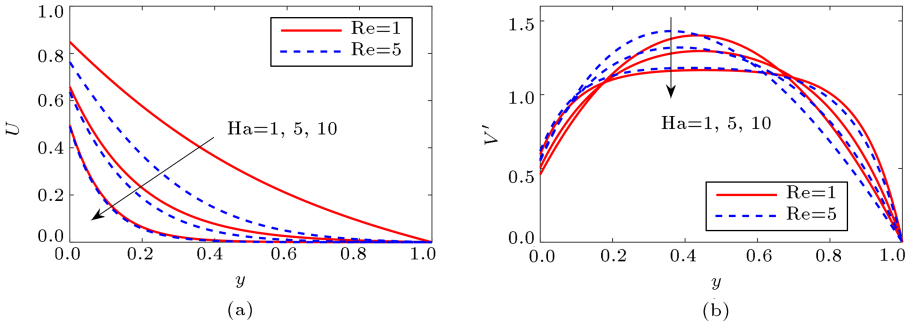

Figure 6. (a) $U(y)$ and (b) $V'(y)$ for Ha with $\lambda = 0.1$, $\beta = 0.1$, and $\phi = 0.05$ for water-Fe_3O_4 nanofluid.

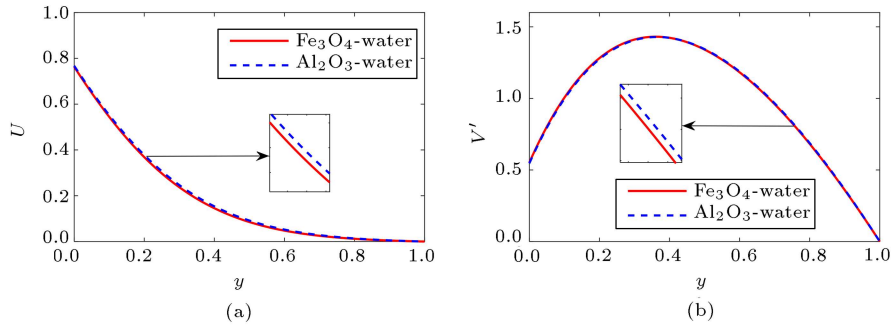

Figure 7. Comparison of different nano particles with water: (a) $U(y)$ and (b) $V'(y)$ when Ha $= 1$, Re $= 1$, $\lambda = 0.1$, $\beta = 0.1$, and $\phi = 0.05$.

slip effects at the lower wall of the channel. $U(y)$ decreases with the increasing values of Re. Decrease in the velocity is the outcome of the inertial forces, which increase with rise in Re as it is expressed as the ratio of inertial to viscous forces. Moreover, an increase in Re decreases the thickness of BL of velocity and increases the magnitude of coefficient for the skin friction in both cases of slip and no-slip at the wall.

Effects of Hartman number, Ha, on $U(y)$ and $V'(y)$ for water-Fe_3O_4 nanofluid are shown in Figure 6(a) and (b), respectively. Figure 6(a) shows reduction in the velocity and BL thickness by increasing the Hartman number for both low and high Reynolds numbers; however, for a large Reynolds number, the velocity profiles shift towards the solid wall. The Hartman number is associated with the resistive force named Lorentz force, which impedes the flow of the fluid. When Hartman number increases, the resistive force also increases, resulting in the decrement of the fluid velocity.

Figure 7(a) and (b) depicts the velocity profiles $U(y)$ and $V'(y)$ for water-Fe_3O_4 and water-Al_2O_3 nanofluids by keeping $\lambda = 0.1$, $\phi = 0.05$, $\beta = 0.1$, Ha $= 1$, and Re $= 5$ fixed. From Figure 7(a), it is observed that the velocity BL for nanofluid with magnetic nanoparticles is lower than the BL for nanofluid with non-magnetic nanoparticles; however, this difference is small. Figure 7(b) also shows that the value of $V'(y)$ for the nanofluid with magnetic nanoparticles is lower than that for nanofluid with non-magnetic nanoparticles. Figure 8(a) and (b) shows the behavior of $U(y)$ and $V'(y)$ for EG-Fe_3O_4 and EG-Al_2O_3 nanofluids by keeping $\phi = 0.05$, $\lambda = 0.1$, $\beta = 0.1$, Ha $= 1$, and Re $= 5$ fixed. A similar behavior

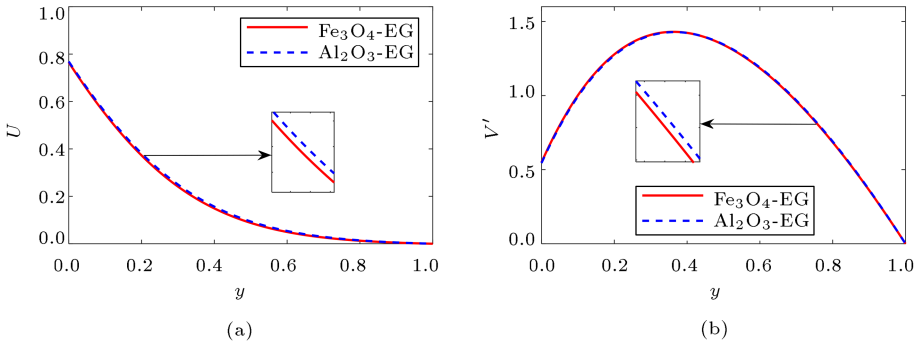

Figure 8. Comparison of different nano particles with Ethylene Glycol (EG), (a) $U(y)$ and (b) $V'(y)$ when Ha = 1, Re = 1, $\lambda = 0.1$, $\beta = 0.1$, and $\phi = 0.05$.

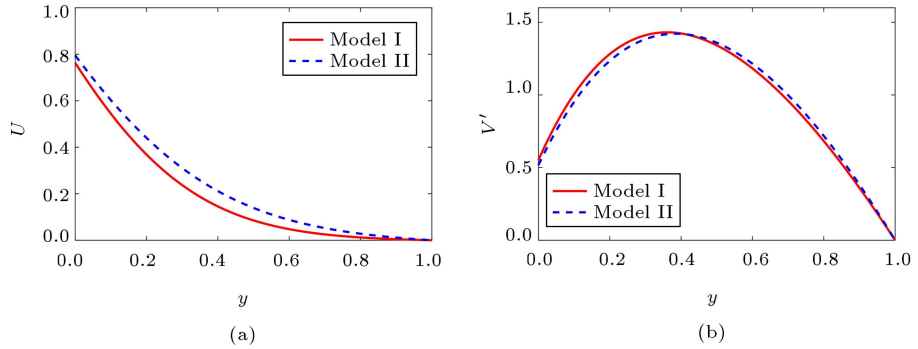

Figure 9. (a) $U(y)$ and (b) $V'(y)$ for two models in case of water-Fe_3O_4 nanofluid with Ha = 1, Re = 1, $\lambda = 0.1$, $\beta = 0.1$, and $\phi = 0.05$.

pattern for $U(y)$ and $V'(y)$ in the case of water-Fe_3O_4 and water-Al_2O_3 nanofluids can be observed.

Figure 9(a) and (b) shows the difference between profiles $U(y)$ and $V'(y)$ for two different models of dynamic viscosity. These figures indicate that there is no major difference in the velocity profiles and the thickness of BL.

The graphs of residuals observed in the LSM are plotted in Figure 10 for different parameters, namely Re and Ha. It is concluded that the residual becomes zero and convergence occurs after the 4th iteration, which shows that the LSM converges more rapidly than Homotopy method.

The comparison results of different methods for $U(y)$ and $V'(y)$ are tabulated in Tables 3 and 4. These tables clearly show that GM outperformed the LSM in terms of numerical solution. The values of $U(0)$ for water-Fe_3O_4 nanofluid in the case of Ha, Re, λ and β and $\phi = 0.05$ are calculated through the LSM and, also, CPU time is calculated and shown in Table 5.

Table 3. Comparison of results of $U(y)$ from the applied methods with Ha = 1, Re = 1, $\lambda = 0.1$, $\beta = 0.1$, and $\phi = 0.05$ for water-Fe_3O_4 nanofluid.

y	NM	LSM	GM
0.0	0.852309	0.8498	0.848292
0.1	0.711011	0.7066	0.704493
0.2	0.583578	0.5781	0.576315
0.3	0.470669	0.4648	0.463272
0.4	0.371929	0.3661	0.364615
0.5	0.286306	0.2810	0.279333
0.6	0.212322	0.2078	0.206159
0.7	0.148303	0.1449	0.143560
0.8	0.092568	0.0903	0.089745
0.9	0.043570	0.0425	0.042663
1.0	0.000000	0.0000	0.000000

6. Conclusion

Having applied the Weighted Residual Methods (WRMs) including Least Square Method (LSM) and Galerkin Method (GM), this study presented a solution to the flow equations of nanofluid in a semi-porous channel through porous media with slip boundary in the presence of a constant magnetic field. The results showed that the difference between the velocity profiles

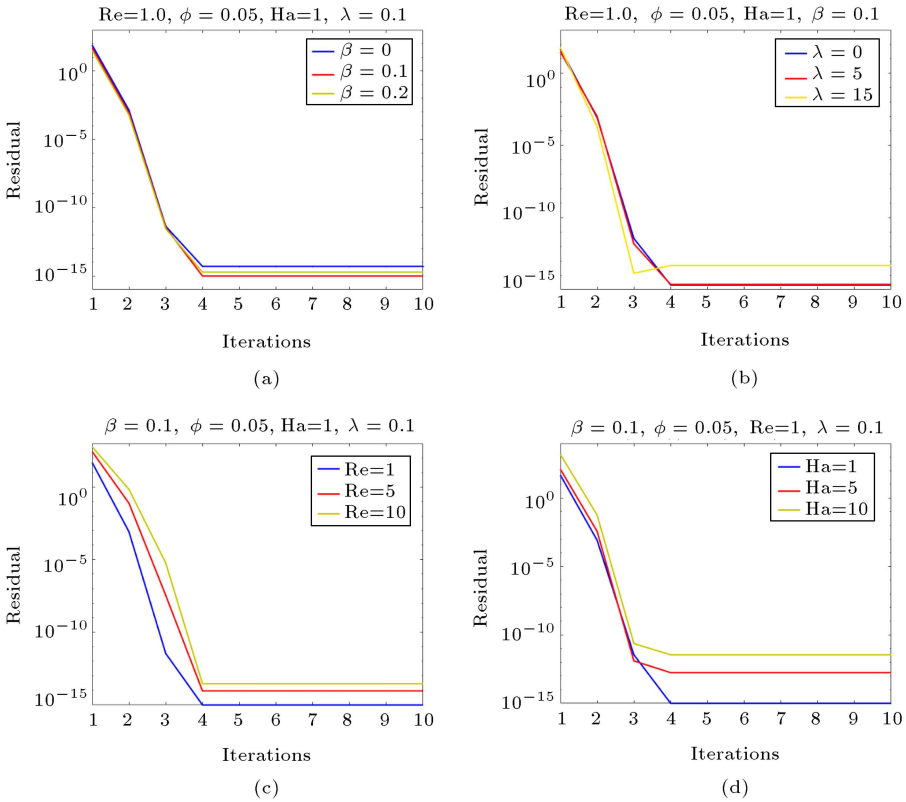

Figure 10. Residual error graphs for different values of the parameters.

Table 4. Comparison of results of $V'(y)$ from the applied methods with Ha = 1, Re = 1, $\lambda = 0.1$, $\beta = 0.1$, and $\phi = 0.05$ for water-Fe_3O_4 nanofluid.

y	NM	LSM	GM
0.0	0.458266	0.458953	0.458616
0.1	0.857286	0.858363	0.857424
0.2	1.142434	1.143709	1.142047
0.3	1.320653	1.321966	1.319919
0.4	1.398393	1.399359	1.397520
0.5	1.381209	1.381366	1.380375
0.6	1.273598	1.272719	1.273053
0.7	1.079062	1.077398	1.079170
0.8	0.800345	0.798638	0.801389
0.9	0.439823	0.438926	0.441415
1.0	0.000000	0.000000	0.000000

was quite small and hence, neglectable. In addition, as the porosity parameter and slip parameter increased, the velocity and thickness of BL decreased. It was also revealed that the velocity BL for the nanofluid with magnetic nanoparticles was lower than that for the nanofluid with non-magnetic nanoparticles.

Table 5. Numerical value of $U(0)$ with Least Square Method (LSM) for different values of Ha, Re, λ, and $\phi = 0.05$ for water-Fe_3O_4 nanofluid.

Ha	Re	λ	β	U (0)	CPU time (s)
1.0	1.0	0.1	0.1	0.8498	64.540230
5.0	–	–	–	0.6595	63.063958
10.0	–	–	–	0.5081	62.796523
1.0	5.0	0.1	0.1	0.7753	62.595650
–	10.0	–	–	0.7247	61.152358
1.0	1.0	0.0	0.1	0.8515	63.528844
–	–	5.0	–	0.7840	64.162391
–	–	15.0	–	0.7062	62.767368
1.0	1.0	0.1	0.0	1.0000	52.313212
–	–	–	0.2	0.7348	64.902356

Acknowledgement

Thanks to the anonymous reviewers for their useful comments which enhanced the final version of the paper.

Nomenclature

A^*, B^*	Constant parameters
q	Transpiration velocity
$\tilde{P}$	Hydrostatic pressure
u, ν	Dimensionless components of velocity vector in x and y directions
$\tilde{u}, \tilde{\nu}$	Velocity vector components in $\tilde{x}$ and $\tilde{y}$ directions
x, y	Dimensionless variables
$\tilde{x}, \tilde{y}$	Spatial coordinates
U, V	Velocity functions
R_i	Residual functions
W_k	Weight functions
c_k	Arbitrary constants
Re	Reynolds number
Ha	Hartmann number
k_1	Permeability of porous medium
B	Magnetic field strength
L	Length of plate
l	Length of slip

Greek symbols

ρ	Fluid density
μ	Dynamic viscosity
ν	Kinematic viscosity
σ	Electrical conductivity
ε	Aspect ratio
λ	Porosity parameter
β	Slip parameter
ϕ	Nanoparticle volume fraction

Subscripts

h	Condition at upper wall
nf	Nanofluid
f	Base fluid
s	Nano-solid particles

References

1. Jafari, A., Zamankhan, P., Mousavi, S.M., et al. "Numerical investigation of blood flow. Part II: In capillaries", *Commun. in Nonlinear Sci. and Numer. Simul.*, **14**(4), pp. 1396–1402 (2009).
2. Goerke, A.R., Leung, J., and Wickramasinghe, S.R. "Mass and momentum transfer in blood oxygenators", *Chem. Engng. Sci.*, **57**, pp. 2035–2046 (2002).
3. Wernert, V., Schäf, O., Ghobarkar, H., et al. "Adsorption properties of zeolites for artificial kidney applications", *Microporous and Mesoporous Materials*, **83**(1–3), pp. 101-113 (2005).
4. Mneina, S.S. and Martens, G.O. "Linear phase matched filter design with causal real symmetric impulse response", *AEU-Int. J. of Elect. and Commun.*, **63**(2), pp. 83-91 (2009).
5. Runstedtler, A. "On the modified Stefan-Maxwell equation for isothermal multicomponent gaseous diffusion", *Chem. Engng. Sci.*, **61**(15), pp. 5021–5029 (2006).
6. Andoh, Y.H. and Lips, B. "Prediction of porous walls thermal protection by effusion or transpiration cooling. An analytical approach", *Appl. Therm. Engng.*, **23**(15), pp. 1974–1958 (2003).
7. Berman, A.S. "Laminar flow in channels with porous walls", *J. of Appl. Phys.*, **24**(9), pp. 1232–1235 (1953).
8. Shekholeslami, M., Ashorynejad, H.R., Domairry, D., et al. "Investigation of the laminar viscous flow in a semi-porous channel in the presence of uniform magnetic field using optimal homotopy asymptotic method", *Sains Malaysiana*, **41**(10), pp. 1281–1285 (2012).
9. Choi, S.U.S., Zhang, Z.G., Yu, W., et al. "Anomalous thermal conductivity enhancement in nanotube suspensions", *Appl. Phys. Lett.*, **79**(14), p. 2252 (2001).
10. Choi, S.U.S. and Eastman, J.A. "Enhancing thermal conductivity of fluids with nanoparticles", *The Proceedings of the 1995 ASME International Mechanical Engineering Congress and Exposition*, ASME, San Francisco, USA, FED 231/MD, **66**, pp. 99–105 (1995).
11. Goharkhah, M. and Ashjaee, M. "Effect of an alternating nonuniform magnetic field on ferrofluid flow and heat transfer in a channel", *J. of Mag. and Magn. Mat.*, **362**, pp. 80–89 (2014).
12. Abbas, Z. and Hasnain, J. "Two-phase magnetoconvection flow of magnetite (Fe_3O_4) nanoparticles in a horizontal composite porous annulus", *Results in Physics*, **7**, pp. 574–580 (2017).
13. Ghasemian, M., Najafian Ashrafi, Z., Goharkhah, M., and Ashjaee, M. "Heat transfer characteristics of Fe_3O_4 ferrofluid flowing in a mini channel under constant and alternating magnetic fields", *Journal of Magnetism and Magnetic Materials*, **381** pp. 158–167 (2015).
14. Sheikholeslami, M., Ganji, D.D., and Rashidi, M.M. "Ferrofluid flow and heat transfer in a semi annulus enclosure in the presence of magnetic source considering thermal radiation", *J. of the Taiwan Inst. of Chem. Eng.*, **47** pp. 6–17 (2015).
15. Soleimani, S., Sheikholeslami, M., Ganji, D.D., et al. "Natural convection heat transfer in a nanofluid filled semi-annulus enclosure", *Int. Commun. in Heat and Mass Trans.*, **39**(4), pp. 565–574 (2012).
16. Sheremet, M.A., Trimbias, R., Grsoan, T., et al. "Natural convection of an alumina-water nanofluid inside an inclined wavy-walled cavity with a non-uniform heating using Tiwari and Das' nanofluid model", *Appl. Math. and Mech.*, **39**(10), pp. 1425–1436 (2018).

17. Siddiqui, A.A. and Sheikholeslami, M. "TiO2-water nanofluid in a porous channel under the effects of an inclined magnetic field and variable thermal conductivity", *Appl. Math. and Mech.*, **39**(8), pp. 1201–1216 (2018).

18. Wakif, A., Boulahia, Z., and Sehaqui, R. "Numerical study of the onset of convection in a Newtonian nanofluid layer with spatially uniform and non uniform internal heating", *J. of Nanofluids*, **6**(1), pp. 136–148 (2017).

19. Wakif, A., Boulahia, Z., and Sehaqui, R. "Numerical analysis of the onset of longitudinal convective rolls in a porous medium saturated by an electrically conducting nanofluid in the presence of an external magnetic field", *Results in Physics*, **7** pp. 2134–2152 (2017).

20. Wakif, A., Boulahia, Z., Ali, F., et al. "Numerical analysis of the unsteady natural convection MHD Couette nanofluid flow in the presence of thermal radiation using single and two-phase nanofluid models for cu-water nanofluids", *Int. J. of Appl. and Comput. Math.*, **4**(3), pp. 1–27 (2018).

21. Wakif, A., Boulahia, Z., and Sehaqui, R. "A semi-analytical analysis of electro-thermo-hydrodynamic stability in dielectric nanofluids using Buongiorno's mathematical model together with more realistic boundary conditions", *Res. in Phys.*, **9**, pp. 1438–1454 (2018).

22. Wakif, A., Boulahia, Z., Mishra, S.R., Rashidi, M.M., and Sehaqui, R. "Influence of a uniform transverse magnetic field on the thermo-hydrodynamic stability in water-based nanofluids with metallic nanoparticles using the generalized Buongiorno's mathematical model", *The Europ. Phys. J. Plus*, **133**(181), pp. 1–16 (2018).

23. Wakif, A., Boulahia, Z., Amine, A., et al. "Magneto-convection of alumina-water nanofluid within thin horizontal layers using the revised generalized buongiorno's model", *Front. in Heat and Mass Trans.*, **12**(3), pp. 1–15 (2019). DOI: 10.5098/HMT.12.3

24. Garoosi, F., Hoseininejad, F., and Rashidi, M.M. "Numerical study of natural convection heat transfer in a heat exchanger filled with nanofluids", *Energy*, **109**, pp. 664–678 (2016).

25. Abbas, T., Ayub, M., Bhatti, M., et al. "Entropy generation on nanofluid flow through a horizontal riga plate", *Entropy*, **18**(6), pp. 1–11 (2016). DOI: 10.3390/e18060223

26. Mohebbi, R. and Rashidi, M.M. "Numerical simulation of natural convection heat transfer of a nanofluid in an L-shaped enclosure with a heating obstacle", *J. of the Taiwan Inst. of Chem. Eng.*, **72**, pp. 70–84 (2017).

27. Bashirnezhad, K., Rashidi, M.M., Yang, Z., et al. "A comprehensive review of last experimental studies on thermal conductivity of nanofluids", *J. of Ther. Anal. and Calor.*, **122**(2), pp. 863–884 (2015).

28. Jha, B.K. and Aina, B. "Magnetohydrodynamic natural convection flow in a vertical micro-porous-annulus in the presence of radial magnetic field", *J. of Nanofluids*, **5**(2), pp. 292–301 (2016).

29. Jha, B.K. and Aina, B. "Role of suction/injection on steady fully developed mixed convection flow in a vertical parallel plate microchannel", *Ain Shams Engng. J.*, **9**(4), pp. 747–755 (2016).

30. Sheikholeslami, M., Hatami, M., and Ganji, D.D. "Analytical investigation of MHD nanofluid flow in a semi-porous channel", *Powd. Tech.*, **246**, pp. 327–336 (2013).

31. Stern, R.H. and Rasmussen, H. "Left ventricular ejection: model solution by collocation, an approximate analytical method", *Comp. in Bio. and Medi.*, **26**, pp. 255–261 (1996).

32. Vaferi, B., Salimi, V., Baniani, D.D., et al. "Prediction of transient pressure response in the petroleum reservoirs using orthogonal collocation", *J. of Petrol. Sci. and Engng.*, **98-99**, pp. 156–163 (2012).

33. Aziz, A. and Bouaziz, M.N. "A least squares method for a longitudinal fin with temperature dependent internal heat generation and thermal conductivity", *Ener. Conver. and Manag.*, **52**(8–9), pp. 2876–2882 (2011).

34. Bouaziz, M.N. and Aziz, A. "Simple and accurate solution for convective-radiative fin with temperature dependent thermal conductivity using double optimal linearization", *Ener. Conver. and Manag.*, **51**(12), pp. 2776–2782 (2010).

35. Abbas, Z., Rahim, T., and Hasnain, J. "Slip flow of magnetite-water nanomaterial in an inclined channel with thermal radiation", *Int. J. of Mech. Sci.*, **122**, pp. 288–296 (2017).

36. Ashmawy, E.A. "Fully developed natural convective micropolar fluid flow in a vertical channel with slip", *J. of the Egyp. Mathe. Soc.*, **23**(3), pp. 563–567 (2015).

37. Abbas, Z., Hasnain, J., and Sajid, M. "MHD two-phase fluid flow and heat transfer with partial slip", *Thermal Science*, **20**, pp. 1435–1446 (2016).

38. Sanyal, D.C. and Sanyal, M.K. "Hydromagnetic slip flow with heat transfer in an inclined channel", *Czech. J. of Phys., B.*, **39**, pp. 529–536 (1989).

39. Finlayson, B.A. and Scriven, L.E. "The method of weighted residuals-A reviews", *Appl. Mech. Reviews*, **19**, pp. 735–748 (1966).

Appendix

Residuals R_1 and R_2 are obtained by the relations shown in Box A.I.

$$R_1(c_1-c_5,y)=-\frac{1}{(1-\phi)^{2.5}\mathrm{Re}A^*}\Bigg(\frac{12(\beta+1)c_3y^2+6(\beta+1)c_2y+2(\beta+1)c_1}{\beta+1}-\frac{1}{\beta+1}\lambda$$

$$\Big(c_3\left((\beta+1)y^4-\beta-y\right)+c_2\left((\beta+1)y^3-\beta-y\right)+c_1\left((\beta+1)y^2-\beta-y\right)-y+1\Big)$$

$$-\Big((1-\phi)^{2.5}\mathrm{Ha}^2B^*(c_3((\beta+1)y^4-\beta-y)+c_2((\beta+1)y^3-\beta-y)+c_1((\beta+1)y^2-\beta-y)-y+1)\Big)/\beta+1\Bigg)$$

$$+(c_3\left((\beta+1)y^4-\beta-y\right)+c_2\left((\beta+1)y^3-\beta-y\right)+c_1\left((\beta+1)y^2-\beta-y\right)-y+1)/(\beta+1)(4\beta+1)$$

$$\Big(c_5(5(4\beta+1)y^4-3(8\beta+3)y^2+4\beta+4y)+c_4(4(4\beta+1)y^3-3(6\beta+2)y^2+2\beta+2y)$$

$$-3(2\beta+2)y^2+6\beta+6y\Big)-\frac{c_3\left(4(\beta+1)y^3-1\right)+c_2\left(3(\beta+1)y^2-1\right)+c_1(2(\beta+1)y-1)-1}{(\beta+1)(4\beta+1)}$$

$$\Big(c_5((4\beta+1)y^5-((8\beta+3)y^3+4\beta y+2y^2+c_4((4\beta+1)y^4-(6\beta+2)y^3+2\beta y+y^2)-(2\beta+2)y^3+6\beta y+3y^2\Big),$$

$$R_2(c_1-c_5,y)=\frac{120(4\beta+1)c_5y+24(4\beta+1)c_4}{4\beta+1}-\frac{1}{4\beta+1}\lambda$$

$$(c_5\left(20(4\beta+1)y^3-6(8\beta+3)y+4\right)+c_4\left(12(4\beta+1)y^2-6(6\beta+2)y+2\right)-6(2\beta+2)y+6)$$

$$\frac{(1-\phi)^{2.5}\mathrm{Ha}^2B^*}{1+4\beta}\Bigg(c_5\Big(20(4\beta+1)y^3-6(8\beta+3)y+4\Big)+c_4\Big(12(4\beta+1)y^2-6(6\beta+2)y+2\Big)-6(2\beta+2)y+6\Big)$$

$$-\Bigg(\begin{array}{l}\frac{c_5\left(20(4\beta+1)y^3-6(8\beta+3)y+4\right)+c_4\left(12(4\beta+1)y^2-6(6\beta+2)y+2\right)-6(2\beta+2)y+6}{(4\beta+1)^2}\\ \Big(c_5\left(5(4\beta+1)y^4-3(8\beta+3)y^2+4\beta+4y\right)+c_4\left(4(4\beta+1)y^3-3(6\beta+2)y^2+2\beta+2y\right)-3(2\beta+2)y^2+6\beta+6y\Big)\\ -\Big(\frac{c_5\left(60(4\beta+1)y^2-6(8\beta+3)\right)+c_4(24(4\beta+1)y-6(6\beta+2))-6(2\beta+2)}{(4\beta+1)^2}\Big)\\ \Big(c_5\left((4\beta+1)y^5-(8\beta+3)y^3+4\beta y+2y^2\right)+c_4\left((4\beta+1)y^4-(6\beta+2)y^3+2\beta y+y^2\right)-(2\beta+2)y^3+6\beta y+3y^2\Big)\end{array}\Bigg)$$

$$\times(1-\phi)^{2.5}\mathrm{Re}A^*$$

Box A.I

Biographies

Zaheer Abbas is an Assistant Professor at the Department of Mathematics, The Islamia University of Bahawalpur, Bahawalpur. He received his PhD in Applied Mathematics from Quaid-I-Azam University Islamabad in 2010. His research interests include Newtonian and non-Newtonian fluids flow, fluid flow in porous medium, heat and mass transfer, magnetohydrodynamics, and fluid dynamics of peristaltic flows.

Jafar Hasnain is an Assistant Professor at the Department of Computer Sciences, Bahria University, Islamabad Campus, Pakistan. He received his PhD in Applied Mathematics from the Islamia University of Bahawalpur, Bahawalpur in 2016. His main interest covers Newtonian and non-Newtonian fluid flows, fluid flow in porous medium, nanofluid, magnetohy-

drodynamics, two-phase flows, heat transfer analysis, chemically reactive fluid flow, etc.

Muhammad Aqeel is a PhD student at the Department of Mathematics, the Islamia University of Bahawalpur, Bahawalpur. He obtained his MS degree in Applied Mathematics from the same department. His main interests cover Newtonian and non-Newtonian fluid flows, fluid flow in porous medium magnetohydrodynamics, heat transfer analysis, etc.

Irfan Mustafa obtained his PhD from the Department of Mathematics and Statistics, International Islamic University Islamabad. His research areas include computational fluid dynamics and stability analysis of fluid flow problem. He is currently working as a lecturer at Allama Iqbal Open University Islamabad, Pakistan.

Abuzar Ghaffari obtained his PhD form the Department of Mathematics, International Islamic University Islamabad. His research area is computational fluid dynamics. He is currently working as an Assistant Professor at University of Education Attock Campus, Pakistan.